In presenting the dissertation as a partial fulfillment of the requirements for an advanced degree from the Georgia Institute of Technology, I agree that the Library of the Institute shall make it available for inspection and circulation in accordance with its regulations governing materials of this type. I agree that permission to copy from, or to publish from, this dissertation may be granted by the professor under whose direction it was written, or, in his absence, by the Dean of the Graduate Division when such copying or publication is solely for scholarly purposes and does not involve potential financial gain. It is understood that any copying from, or publication of, this dissertation which involves potential financial gain will not be allowed without written permission.

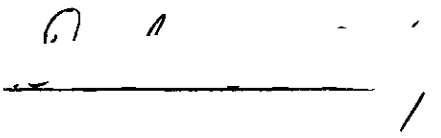

7/25/68

MEAN L-FLUORESCENCE YIELDS AND RELATIVE L X-RAY INTENSITIES IN THE REGION Z = 55 TO 65

A THESIS

Presented to

The Faculty of the Division of Graduate

Studies and Research

by

Dale Wendel Nix

In Partial Fulfillment

Of the Requirements for the Degree

Master of Science in Chemistry

Georgia Institute of Technology

March, 1972

MEAN L-FLUORESCENCE YIELDS AND RELATIVE L X-RAY INTENSITIES IN THE REGION Z = 55 TO 65

Approved:

Chairman

Date approved by Chairman: FEB 25 1972

ACKNOWLEDGEMENTS

It gives me great pleasure to recognize the people whose support made this research possible.

I should like to thank my thesis advisor, Professor R. W. Fink, who suggested this research project and was an invaluable aid in helping me write the thesis.

I would also like to thank Drs. J. C. McGeorge and J. S. Hansen for providing valuable advice, aid, and assistance in all aspects of this research project.

I am also greateful to the members of the reading committee, Drs. G. G. Eichholz and J. A. Bertrand, for manuscript suggestions.

Dr. M. L. Hyder of the Savannah River Laboratory provided the electrodeposited sources of Pm^{238} and Cm^{244}.

I wish to express by sincere appreciation to my parents for instilling within me perseverance and for making it possible to obtain a college education.

I am deeply indebted to my wife, Susan, for encouragement in completing this work and for the typing of this thesis.

This research project was supported by AEC Contract AT(40-1)-3346 as part of a larger program in nuclear spectroscopy-nuclear chemistry.

TABLE OF CONTENTS

LIST OF TABLES

LIST OF ILLUSTRATIONS

SUMMARY

This research involves an experimental study of the ratio (I_L/I_K) of the intensity of the L x rays (I_L) to the intensity of the K x rays (I_K) emitted from radioactive sources. These measurements have been made for the first time with high resolution Si(Li) and Ge(Li) x-ray detectors. From this ratio values of the mean L-shell fluorescence yield ($\bar{\omega}_L$) have been determined for elements with Z = 55, 56, 57, 59, and 65. The ratio (I_{K_α}/I_{L_ℓ}) of the intensity of the $L_3 - M_{4,5}$ x-ray transition (I_{L_α}) to the intensity of the $L_3 - M_1$ x-ray transition (I_{L_ℓ}) is also deduced from the L x-ray spectra in the region $55 \leq Z \leq 94$. A complete set of equations have been developed to calculate the mean L-shell fluorescence yield, $\bar{\omega}_L$, and the primary vacancy distribution for the decay of any nuclide.

The present study is significant because:

1) Measurements of L-subshell fluorescence yields are very difficult at medium and low atomic numbers ($Z < 65$). Thus, studies of mean L-shell fluorescence yields, $\bar{\omega}_L$, coupled with theoretical calculations and complete experimental studies at higher Z ($Z \geq 65$), might enable one to draw some conclusions about L-subshell fluorescence yields in the

region where these quantities cannot be measured accurately.

2) Agreement among previous workers working at much lower resolution has been very poor.

3) Recent advances in the field of radiation detection, source preparation, and nuclear physics theory and experiment have made revision of previous work desirable.

CHAPTER I

INTRODUCTION

1.1 Historical Background

The emission of characteristic x rays was associated with radioactivity soon after its discovery[1]. However, it was not until 1925 that the Auger effect was discovered[2]. Since two competing processes for filling vacancies have become known, namely, radiative and nonradiative transitions, measurements of the probability for radiative or nonradiative transitions began in 1925.

Auger was the first to measure the probability that a vacancy in the L shell is filled by a radiative transition, defined as the mean L-shell fluorescence yield ($\bar{\omega}_L$) for argon[1]. After the work of Auger, Lay in 1934 undertook a systematic measurement of $\bar{\omega}_L$ values by fluorescent excitation of foils or gaseous targets for many of the elements of $40 \leq Z \leq 92$[3]. More recent systematic studies (with radioactive sources) of $\bar{\omega}_L$ and of ω_{KL}, a mean fluorescence yield composed of the L_2 and L_3 subshell yields and observed by means of K-L x-ray coincidences, were undertaken by Hohmuth, Muller, and Schintlmeister[4], and Hohmuth and Winter[5]. Jopson, Mark, Swift, and Williamson[6], carried out extensive measurements of a mean fluorescence yield ω_{KL} with fluorescent

excitation of thin foils and K-L x-ray coincidences. Other authors have reported values for a limited range of Z[7]. Literature values of $\bar{\omega}_L$ and ω_{KL} pertaining to the present investigation are discussed below in Sect. 3.3 and appear in Table 4.

1.2 Objectives and Applications

Advances in the fields of x-ray detection by semiconductors[8,9,10], of source preparation, and in knowledge of radioactive decay schemes enable one to measure mean L-shell fluorescence yields with greater accuracy than heretofore possible. High flux reactors or accelerators facilitate the production of high-specific-activity or carrier-free radioactive sources. New theoretical calculations[11] of the probability of K and L electron capture and of conversion coefficients as well as recent accurate measurements of such decay scheme quantities as branching ratios[13,14], and a reevaluation of the quantity n_{KL}, the number of L-shell vacancies produced in the decay of a K-shell vacancy, enable one to determine more accurate values of $\bar{\omega}_L$.

Very accurate measurement of L-subshell fluorescence yields are impossible at medium and low atomic numbers ($Z < 65$), because of the difficulty of resolving the K_{α_1} (K-L_3) and K_{α_2} (K-L_2) x ray transitions. However, studies of $\bar{\omega}_L$, coupled with theoretical calculations, and experimental studies of the L-subshell fluorescence and Coster-Kronig yields at

higher Z ($Z > 65$) should allow one to draw some conclusions about L-subshell yields in the region where these quantities cannot be measured accurately ($Z < 65$).

The objectives of this work are to measure $\bar{\omega}_L$ for elements of atomic numbers 55, 56, 57, 59, and 65 with greater accuracy than previously possible and, where possible, to measure the x-ray intensity ratio I_{L_α}/I_{L_ℓ}, where I_{L_α} is the intensity of the L_α (L_3-$M_{4,5}$) x ray transition and I_L is the intensity of the L_ℓ (L_3-M_1) x ray transition.

Accurate values of $\bar{\omega}_L$ are required in the study of certain types of branching ratios and conversion coefficients. Gamma transitions with energies just above the L-shell binding energy cannot be studied by detecting the L conversion electrons or γ rays. The electrons are very low in energy and very few γ rays are emitted, since such transitions are very highly converted. Thus some other radiation associated with the process must be studied. If the low energy transition is fed by a γ transition (γ_1), the L x rays can be detected in coincidence with the first γ transition, γ_1. The product of the branching ratio and the L-shell conversion coefficient will be related to $\bar{\omega}_L$ by the equation:

$$I_L(\gamma_1) / C_{\gamma_1} = \bar{\omega}_L \, f \, [\alpha_L / (1+\alpha_T)] \qquad (1)$$

where $I_L(\gamma_1)$ is the intensity of the L x rays in coincidence with the first γ ray, γ_1; C_{γ_1} is the number of γ_1 counts in

the gate; $\underline{f}$ is the branching ratio for the low energy transition; and α_L and α_T are the L shell and total conversion coefficients, respectively.

Precise calculations of photon transport processes necessary to compute dose build-up factors and design optimum shielding[17] require an accurate determination of the contribution of secondary radiation. Terms which compute this contribution require accurate values of $\bar{\omega}_L$.

Lithium-drifted silicon [Si(Li)] x-ray detectors are commonly used in x-ray fluorescence and microprobe analysis[15]. As Si(Li) x-ray detectors have low efficiency above about 30 keV, they are limited to the detection of K x rays from low Z elements or of L x rays. When absolute L x ray counting is used or absolute L x-ray standards are made, it is necessary to calculate quantitatively the abundance of the desired element using values of $\bar{\omega}_L$[16].

The accurately determined (±10 per cent) x-ray intensity ratio I_L/I_K can be used to calibrate approximately the detection efficiency for photon detection devices. Emission rates such as those given in Table 1 (p. 13) can be calculated for the L x rays by using the emission rate for the K shell and the I_L/I_K intensity ratio measured in the present work.

1.3 Terminology

There are several types of yields which are defined for the K and L shell. The K shell has two yields associated with it. These two yields are the K-shell fluorescence yield (ω_K) and the K-shell Auger yield (a_K). The K-shell fluorescence yield is defined as the probability that a vacancy in the K shell of an atom is filled by a radiative transition (K x ray). The Auger yield is defined as the probability that a vacancy in the K shell of an atom is filled by a nonradiative transition (Auger transition, denoted as K-XY where X and Y denote any electronic subshell higher than the K shell).

In the L shell there are nine different yields; of these, there are three Auger yields and three fluorescence yields corresponding to the three L subshells. In addition there are three Coster-Kronig yields. The Auger yield (a_i) is the probability that a vacancy in the ith subshell of an atom is filled by a nonradiative transition from a higher major shell (Auger Transition). The fluorescence yield (ω_i) is the probability that a vacancy in the ith subshell is filled by a radiative transition (L x ray); hence, $\omega_i = 1-a_i$. The Coster-Kronig yield (f_{ij}) is the probability of occurrence of the Coster-Kronig transition $L_i - L_j$.

There are also two mean yields associated with the L shell. These are the mean fluorescence yield ($\bar{\omega}_L$) and the mean Auger yield ($\bar{a}_L$) These are defined as the probability

that a vacancy in any L subshell of an atom is filled by a radiative transition or a nonradiative transition, respectively. The mean fluorescence yield is given in terms of the subshell yields as:

$$\bar{\omega}_L = N_1[\omega_1+f_{12}\omega_2+(f_{13}+f_{12}f_{13})\omega_3]+N_2(\omega_2+f_{23}\omega_3)+N_3\omega_3 \qquad (2)$$

where N_1, N_2, and N_3 are the normalized primary vacancy distributions of the L_1, L_2, and L_3 subshells, respectively ($N_1 + N_2 + N_3 = 1$).

Further details of the interrelation of the above yields can be found in a review by Fink, Jopson, Mark and Swift[18].

1.4 Basis of the Experimental Method

The relative intensities of K-shell x rays (I_K) and L-shell x rays (I_L) were measured in the present work for several isotopes that create vacancies by electron capture (EC) and/or internal conversion (IC) processes. The equations which relate I_K and I_L to the mean L fluorescence yield ($\bar{\omega}_L$) are as follows:

$$I_K = N_o\omega_K N_{K(T)} = N_o\omega_K[\sum_n N_{K(n)} + \sum_{i,j} N_{K(i,j)}] \qquad (3)$$

$$I_L = N_o\bar{\omega}_L N_{L(T)} = N_o\bar{\omega}_L[\sum_n N_{L(n)} + \sum_{i,j} N_{L(i,j)}] \qquad (4)$$

where

$$N_{K(n)} = f_{(n)}P_{K(n)} \qquad (5)$$

$$N_{K(i,j)} = b_{(i,j)}[\alpha_K/(1+\alpha_T)]_{(i,j)} \tag{6}$$

$$N_{L(n)} = f_{(n)}P_{L(n)} + n_{KL}N_{K(n)} \tag{7}$$

and

$$N_{L(i,j)} = b_{(i,j)}[\alpha_L/(1+\alpha_T)]_{(i,j)} + n_{KL}N_{K(i,j)} \tag{8}$$

where N_o is the disintegration rate of the source; ω_K is the K-shell fluorescence yield; $N_{K(T)}$ and $N_{L(T)}$ are the total number of K-shell and L-shell vacancies, respectively, produced per disintegration due to electron capture and/or internal conversion*; $N_{K(n)}$ and $N_{L(n)}$ are the number of K-shell and L-shell vacancies, respectively, produced by electron capture to the level of the daughter indicated by the index n, where n is energy (in keV) of the level in the daughter nucleus fed by electron capture decay; $N_{K(i,j)}$ and $N_{L(i,j)}$ are the numbers of K-shell and L-shell vacancies, respectively, produced by a γ transition between levels i and j in the daughter nucleus where i and j are the values of the energy (in keV) of the initial and final energy levels, respectively, in the daughter

*The meanlife of a L-subshell vacancy is less than 10^{-14} sec while the lifetime of a nuclear state is greater than 10^{-10} sec in the presently studied cases. Thus, vacancies produced by electron capture or internal conversion are filled long before supplementary vacancies can be produced by internal conversion.

nucleus; $f_{(n)}$ is the fraction of total electron capture transitions leading to level $\underline{n}$ in the daughter nucleus; $P_{K(n)}$ and $P_{L(n)}$ are the probabilities of K- and L-electron capture, respectively, for decay to level $\underline{n}$ in the daughter nucleus; $b_{(i,j)}$ is the probability that a specific level $\underline{i}$ in the daughter nucleus deexcites by a γ transition to level $\underline{j}$; $[\alpha_K/(1+\alpha_T)]_{(i,j)}$ and $[\alpha_L/(1+\alpha_T)]_{(i,j)}$ are the probabilities that a K-shell or L-shell vacancy, respectively, is produced by internal conversion of the transition between levels $\underline{i}$ and $\underline{j}$ in the daughter nucleus, where α_K, α_L, and α_T are the K-shell, L-shell, and total conversion coefficients, respectively, and n_{KL} is the number of L-shell vacancies produced in the filling of a K-shell vacancy[18],

$$n_{KL} = \omega_K[I_{K\alpha}/I_K]+a_K\{[2(K\text{-}LL)+(K\text{-}LX)]/\Sigma\text{Auger}\} \qquad (9)$$

where $I_{K\alpha}/I_K$ is the intensity ratio of K_α x rays to total K x rays; a_K is the K Auger yield $(1-\omega_K)$; K-LL is the probability that a K-shell vacancy is filled by an L-shell electron with the energy difference transferred to an ejected L-shell electron; K-LX is the probability that a K-shell vacancy is filled by an L-shell electron with the energy difference transferred to an ejected X-shell electron (X stands for M, N, O, etc.), and Σ Auger is the sum of the Auger electron intensities.

The ratio of eqs. 4 and 3 yields an expression for $\bar{\omega}_L$:

$$\bar{\omega}_L = \omega_K (I_L/I_K)[N_{K(T)}/N_{L(T)}] \qquad (10)$$

in terms of the experimentally measured ratio I_L/I_K; the K-shell fluorescence yield ω_K, and the ratio of total L-shell and K-shell vacancies. A detailed calculation of $\bar{\omega}_L$ for a typical case, Ce^{139g}, is given in Appendix A.

CHAPTER II

EXPERIMENTAL

2.1 Source Preparation

Thin uniform sources of Ba^{133g}, Cs^{137}, Ce^{139g}, Ce^{141}, Pm^{145}, Dy^{159}, W^{181}, and Bi^{207} were prepared by insulin spreading of carrier-free, solids-free radioactive solutions obtained from New England Nuclear Corporation, Boston, Massachusetts. The solutions were drop evaporated onto 0.025 mm thick Mylar sheets. A drop of 1:20 insulin-water provided a low-surface-tension substrate of area approximately equal to 0.25 cm^2. The radioactive solutions were deposited with a micropipet directly onto the insulin-spread area and allowed to dry under a heat lamp. Typical source strengths were in the range of 1 - 5 microcuries.

The $_{94}Pu^{238}$ and $_{96}Cm^{244}$ sources (decaying to Z = 92 and 94, respectively) used in the determination of I_{L_α}/I_{L_ℓ} were received as a loan from the Savannah River Laboratory at Aiken, South Carolina. These sources were prepared by electrodeposition of 1.00 μCi of Pu^{238} and 1.37 μCi of Cm^{244} (November 1968) on thin nickel discs. The active diameter of the radioactive sources were 1.50 cm. The fluorescently-excited x-ray intensities from the nickel were minimal and their presence was not disturbing.

These nuclides were chosen because they produce vacancies in both the K and L shell by the electron capture and/or internal conversion processes.

2.2 Experimental Equipment

Two separate determinations of the ratio I_L/I_K, for Ba^{133g}, Cs^{137}, Ce^{139g}, and Ce^{141}, were made, each with a different experimental system. The first determination of the ratio I_L/I_K was undertaken using a high resolution (325 eV full-width a half-maximum (FWHM) at 6.4 keV), cooled lithium-drifted germanium (Ge(Li)) detector with an active depth of 5 mm and an active diameter of 6 mm, a Tennelec TC-200 linear amplifier, a TC-250 biased amplifier and stretcher, and a RIDL 400-channel analyzer.

The second determination of the ratio I_L/I_K for all the nuclides given in Table 2, was undertaken using a high resolution (185 eV FWHM at 5.9 keV), cooled lithium-drifted silicon detector (active depth of 5 mm, active diameter of 6 mm) fitted with a "pulsed-optical" feedback preamplifier, a Tennelec TC-202-BLR linear amplifier with baseline restoration, and a 2048-channel Nuclear Data model 2200 analyzer. Both detectors employed cooled field-effect transistors and charge-sensitive preamplifiers.

The two independent systems are used to provide a consistency check.

2.3 Detection Efficiency

Absolutely calibrated radioactive photon sources, provided by the International Atomic Energy Agency, Vienna, (IAEA)* were used to determine the detection efficiency. The relative efficiencies of the Ge(Li) and Si(Li) detectors were measured at distances of 3.175 cm and 1.27 cm, respectively, between the centered source and beryllium window.

The relative detection efficiency $\epsilon_{(E)}$ for photons of energy E in a given geometry is given by:

$$\epsilon_{(E)} = C_E/(N_E N_o) \tag{11}$$

where C_E is the number of counts detected in the photopeak of energy E; N_E is the number of photons of energy E emitted per decay, and N_o is the disintegration rate per second of the standard source.

The standard sources used in the present work are listed in Table 1 with their respective photon energies E and emission probabilities N_E.

The absolute detection efficiency at 3.30 keV was determined with an open Am^{241} source, the M x-ray emission rate of which had been previously determined using a multiwire propane-filled gas proportional counter[19].

*A complete description of these sources is given in Ref. 9.

Table 1. Standardization Sources

Nuclide	Daughter	Photon Energy (keV)	Photons Emitted Per Decay
$_{95}Am^{241}$	$_{93}Np^{237}$	3.30	0.0635±0.006*
		13.9	0.135 ±0.003
		17.8	0.202 ±0.004
		20.8	0.050 ±0.001
		26.4	0.025 ±0.002
		59.54	0.359 ±0.006
$_{27}Co^{57}$	$_{26}Fe^{57}$	6.46	0.553 ±0.015
		14.36	0.095 ±0.002
		121.97	0.856 ±0.003
$_{55}Cs^{137}$	$_{56}Ba^{137}$	32.1	0.0567±0.002
		36.5	0.0134±0.001
$_{25}Mn^{54}$	$_{24}Cr^{54}$	5.47	0.250 ±0.002
$_{39}Y^{88}$	$_{38}Sr^{88}$	14.4	0.6340±0.0032

*All values are taken from Ref. 10.

Figs. 1 and 2 give the relative full-energy-peak detection efficiencies of the Ge(Li) and Si(Li) detectors, respectively, as a function of photon energy. These curves show typical efficiency responses of x-ray detectors. The drop-off at low energy is due to the absorption of the photons in air, the beryllium window, the gold contact layer, and dead silicon or germanium layer, while the drop-off at high energy is due to the decrease in the photo-electric cross section at higher energy. The discontinuity at the top of the germanium efficiency response is due to the escape of K x rays from the active volume of the detector.

Interpolation between the efficiency points determined at the calibration energies was made following the criteria set forth earlier by Freund, Hansen, Karttunen, and Fink[8], Hansen[9], and Hansen, McGeorge, Freund, Schmidt-Ott, Nix, Unus, and Fink[10].

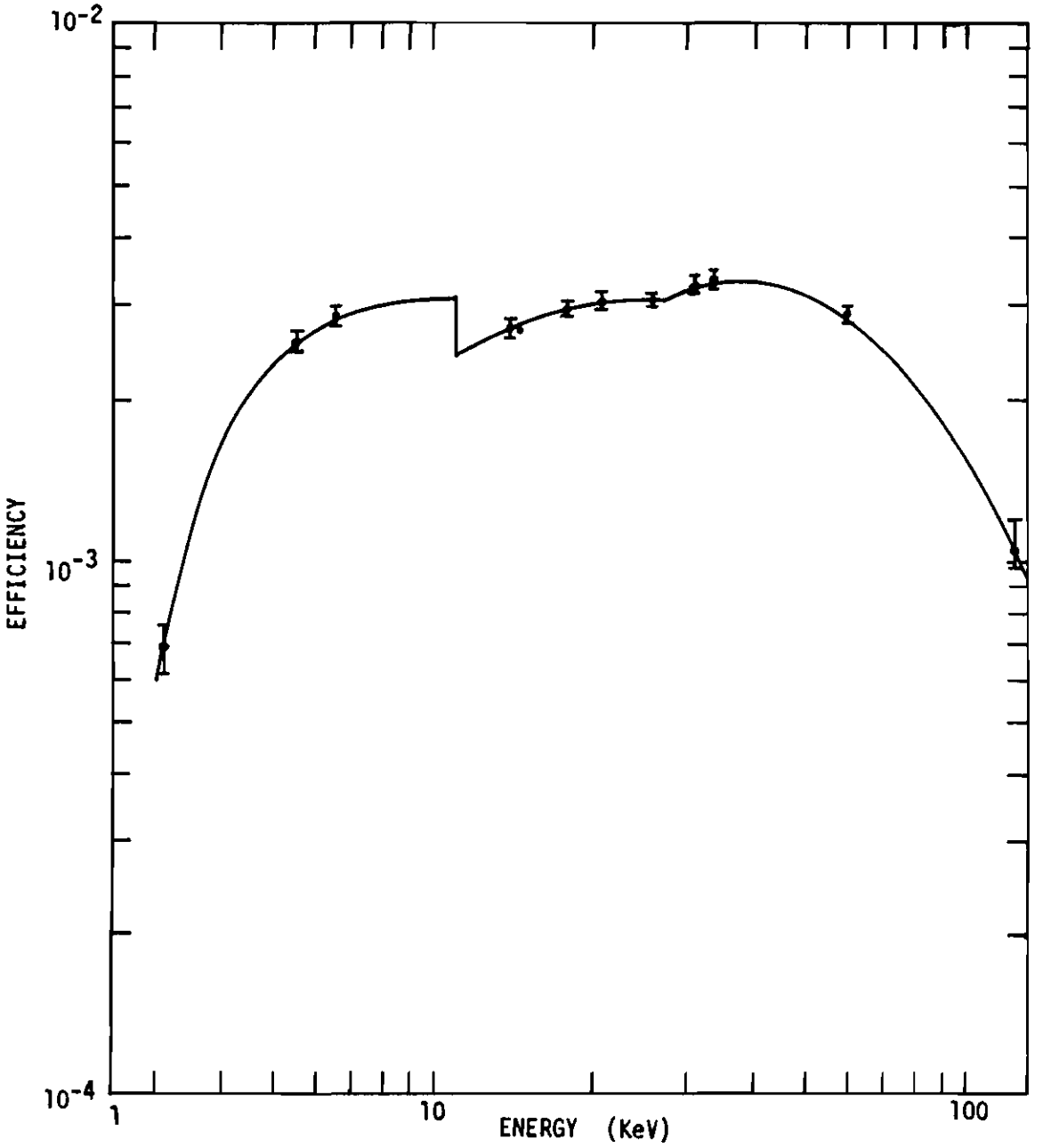

Fig. 1. Efficiency of the Ge(Li) Detector Used in the Present Work.

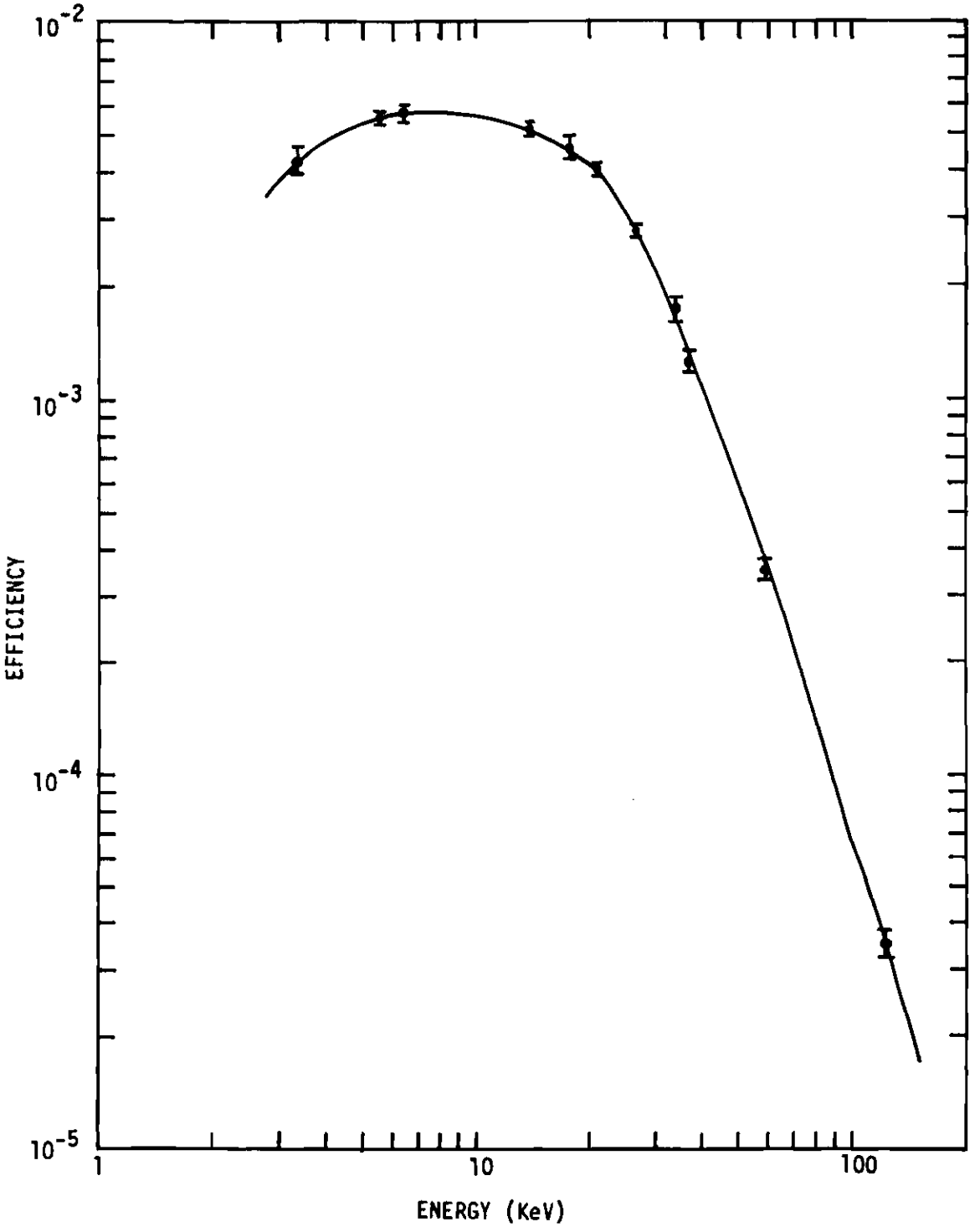

Fig. 2. Efficiency of the Si(Li) Detector Used in the Present Work.

CHAPTER III

RESULTS AND DISCUSSION

3.1 Evaluation of the Ratio I_L/I_K

Spectra were taken for all nuclides listed in Table 2. Several typical spectra are presented in Fig. 3.

The ratio of I_L/I_K was determined by the equation:

$$I_L/I_K = \frac{[(C_{L_\ell}/\epsilon_{L_\ell}) + (C_{L_\alpha}/\epsilon_{L_\alpha}) + (C_{L_\beta}/\epsilon_{L_\beta}) + (C_{L_\gamma}/\epsilon_{L_\gamma})]}{[(C_{K_\alpha}/\epsilon_{K_\alpha}) + (C_{K_{\beta_1'}}/\epsilon_{K_{\beta_1'}}) + (C_{K_{\beta_2'}}/\epsilon_{K_{\beta_2'}})]} \quad (12)$$

where the quantities C_{L_ℓ}, C_{L_α}, C_{L_β}, C_{L_γ}, C_{K_α}, $C_{K_{\beta_1'}}$, and $C_{K_{\beta_2'}}$ and the quantities ϵ_{L_ℓ}, ϵ_{L_α}, ϵ_{L_β}, ϵ_{L_γ}, ϵ_{K_α}, $\epsilon_{K_{\beta_1'}}$, and $\epsilon_{K_{\beta_2'}}$ are the respective counting rates and detection efficiencies for the L_ℓ, L_α, L_β, L_γ, K_α, $K_{\beta_1'}$, and $K_{\beta_2'}$ x-ray groups. The above counting rates were computed after subtracting the continuum beneath the peaks. The continuum was subtracted in an identical manner in the determination of the efficiency, in order to minimize systematic errors in the estimation of the true counting rates.

The results of the determination of I_L/I_K from eq. 12 are shown in Table 2, where the error limits are twice the

Table 2. The Ratio, I_L/I_K, for Several Nuclides

Nuclide	Daughter	I_L/I_K
$_{56}Ba^{133g}$	$_{55}Cs^{133}$	0.114±0.011
$_{55}Cs^{137}$	$_{56}Ba^{137}$	0.110±0.011
$_{58}Ce^{139g}$	$_{57}La^{139}$	0.139±0.014
$_{58}Ce^{141}$	$_{59}Pr^{141}$	0.139±0.014
$_{64}Gd^{153}$	$_{63}Eu^{153}$	0.174±0.017
$_{66}Dy^{159}$	$_{65}Tb^{159}$	0.213±0.021
$_{74}W^{181}$	$_{73}Ta^{181}$	0.344±0.034 *
$_{83}Bi^{207}$	$_{92}Pb^{207}$	0.528±0.053 *

*These are tentative values. Final values will be published later.

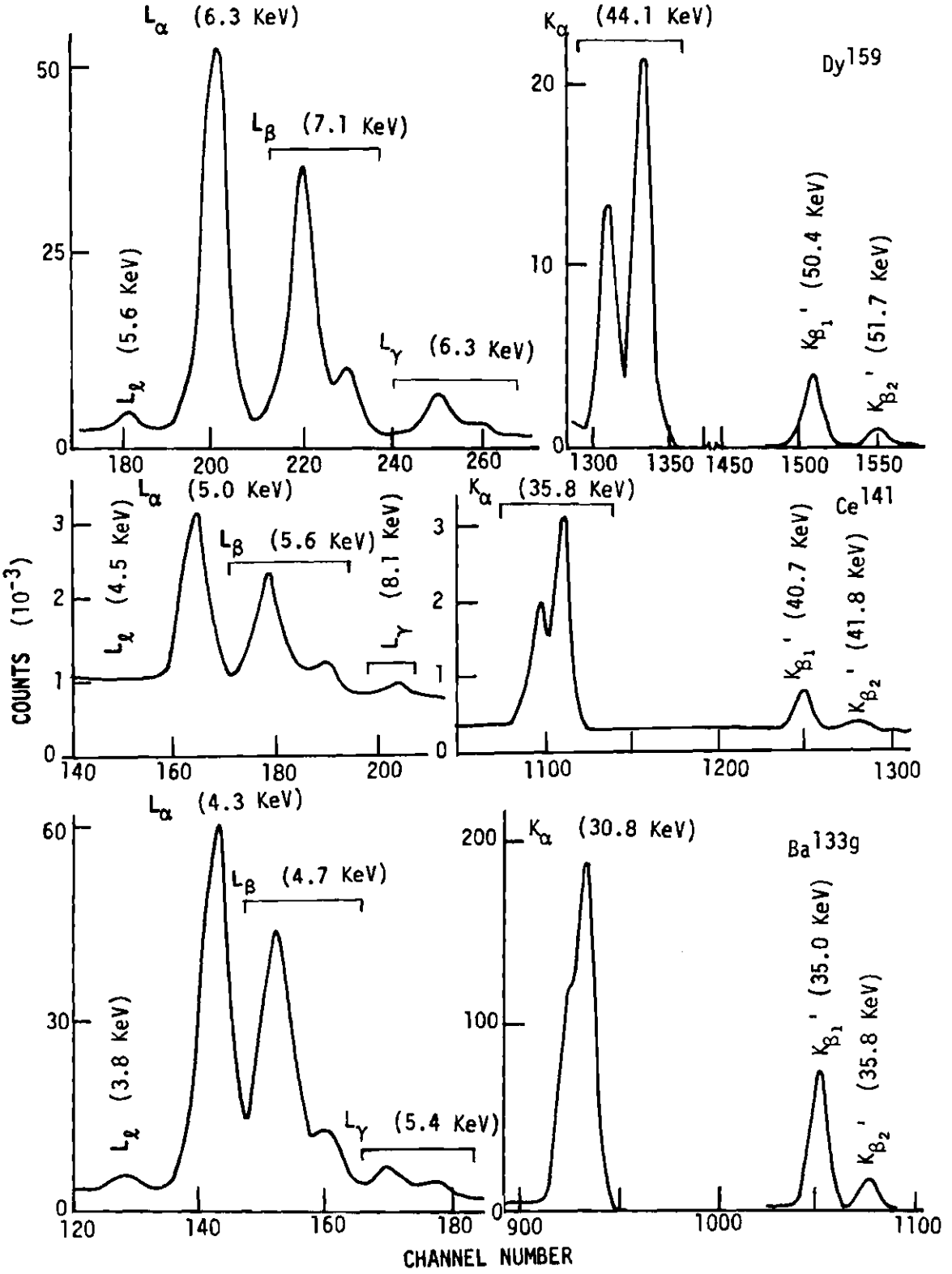

Fig. 3. Typical K and L X-Ray Spectra of Ba^{133g}, Ce^{141}, and Dy^{159} .

standard deviation (95 per cent confidence level), and arise mainly from the uncertainties in the efficiencies. The total number of counts were large for both K and L x rays; therefore, negligible errors were contributed by the counting statistics.

3.2 Evaluation of the Mean L-Shell Fluorescence Yield, $\bar{\omega}_L$

Mean L-shell fluorescence yields were evaluated using eqs. 3 - 8, and 10 given in Sect. 1.4. The values for the relative contributions to K-shell and L-shell vacancies from electron capture, $N_{K(n)}$ and $N_{L(n)}$, and/or internal conversion, $N_{K(i,j)}$ and $N_{L(i,j)}$, are given in Table 3. In addition the total number of vacancies for the K shell $N_{K(T)}$, L shell $N_{L(T)}$, and $\bar{\omega}_L$ are also given for Ba^{133g}, Cs^{137}, Ce^{139g}, Ce^{141}, and Dy^{159}.

The computation of $\bar{\omega}_L$ can be simplified by neglecting contributions to the vacancy production made by weak electron capture branches, and low intensity γ transitions. Examples of these simplifications are the omission of the electron capture branch to the 160.5 keV level in Cs^{133} from the decay of Ba^{133g}, the omission of the electron capture branch to the 348 and 135.5 keV levels in Tb^{159} from the decay of Dy^{159}, and the omission of the 54 keV γ transition in the decay of Ba^{133g}.

The uncertainty in $\bar{\omega}_L$ is due primarily to uncertainties in the measured ratio I_L/I_K (Table 2). The uncertainty in the ratio $N_{K(T)}/N_{L(T)}$, due to the errors in $f_{(n)}$, $b_{(i,j)}$,

Table 3. Evaluation of Quantities Used in the Determination of the Mean L-Shell Fluorescence Yield, $\bar{\omega}_L$

Nuclide	Daughter	n or i,j	$N_{K(n)}$ or $N_{K(i,j)}$ [a]	$N_{L(n)}$ or $N_{L(i,j)}$ [b]	$\bar{\omega}_L$	Calculated from Data in Refs.
$_{56}Ba^{133g}$	$_{55}Cs^{133}$	437	0.573	0.736		11,12,13
		384	0.111	0.125		
		437, 382	0.108	0.111		
		437, 160.5	0.003	0.004		
		437, 81	0.013	0.014		
		382, 81	0.007	0.007		
		382, 0	0.002	0.002		
		160.5, 81	0.037	0.038		
		160.5, 0	0.002	0.002		
		81, 0	0.455	0.475		
		Total	1.31	1.51	0.089±0.013	
$_{55}Cs^{137}$	$_{56}Ba^{137}$		0.077	0.082	0.093±0.012	20
$_{58}Ce^{139g}$	$_{57}La^{139}$	166	0.730	0.862		See Appendix A
		166, 0	0.175	0.178		
		Total	0.905	1.04	0.110±0.015	
$_{58}Ce^{141}$	$_{59}Pr^{141}$	145, 145	0.182	0.188	0.123±0.017	21

(Continued)

Table 3. Evaluation of Quantities Used in the Determination of the Mean L-Shell Fluorescence Yield, $\bar{\omega}_L$ (Continued)

Nuclide	Daughter	n or i,j	$N_{K(n)}$ or $N_{K(i,j)}$ [a]	$N_{L(n)}$ or $N_{L(i,j)}$ [b]	$\bar{\omega}_L$	Calculated from Data in Refs.
$_{66}Dy^{159}$	$_{65}Tb^{159}$	58	0.214	0.223		12,13,14
		0	0.590	0.610		
		58, 0	0.204	0.207		
		Total	1.01	1.04	0.194±0.027	

(a) Final tabulations for each nuclide in the column will be $N_{K(T)}$.

(b) Final tabulations for each nuclide in the column will be $N_{L(T)}$.

$P_{N(n)}$, $P_{L(n)}$, $[\alpha_K/(1+\alpha_T)]_{(i,j)}$, and $[\alpha_L/(1+\alpha_T)]_{(i,j)}$, contributes an uncertainty of 3 to 5 per cent to the total error limits of $\bar{\omega}_L$. The above uncertainties were added linearly. The final error limits on $\bar{\omega}_L$ reflect a 95 per cent confidence level (ie, twice the standard deviation).

3.3 Discussion of $\bar{\omega}_L$

Table 4 lists the experimentally determined values of the mean L-shell fluorescence yield $\bar{\omega}_L$ and the mean fluorescence yield of the L shell following K x-ray emission, ω_{KL}, which is a special case of mean L-shell fluorescence yield*. Although the primary vacancy distribution (N_1: N_2: N_3) is dependent upon the mode of vacancy production, it is nevertheless possible to compare values of the mean L-shell fluorescence yield, $\bar{\omega}_L$.

Even though very few primary vacancy distributions for experiments reported in the literature are exactly the same as those in the present work, it is possible to make a few comments on the agreement and disagreement among certain experiments:

1) The difference in the respective ratios of N_1:

*The quantity ω_{KL} represents a linear combination of the L_2 and L_3 subshell fluorescence yields; ie, $\omega_{KL}=N_2\omega_2+(N_2f_{23}+N_3)\omega_3$, where N_2 and N_3 represent the relative primary vacancy distribution (ie. $N_1=0$) and f_{23} represents the probability for the occurance of the Coster-Kronig transition L_2-L_3 (see Ref. 18).

Table 4. Comparison of Previous Work on $\bar{\omega}_L$ and ω_{KL} with the Present Work

Z	$\bar{\omega}_L$	ω_{KL}	$N_1 : N_2 : N_3$	Reference
55	0.089±0.013		0.252: 0.269: 0.479	Present
56	0.093±0.012		0.239: 0.275: 0.486	Present
	0.148		0.167: 0.333: 0.500	3
57	0.110±0.015		0.259: 0.266: 0.475	Present
	0.158		0.167: 0.333: 0.500	3
	0.092±0.007		0.28 : 0.26 : 0.46	4
		0.15 ±0.02	0.00 : 0.35 : 0.65	6
		0.123±0.022	0.00 : 0.35 : 0.65	22
59	0.123±0.017		0.233: 0.284: 0.483	Present
	0.167		0.17 : 0.33 : 0.50	3
		0.16 ±0.02	0.00 : 0.36 : 0.64	6
		0.09 ±0.01	0.00 : 0.36 : 0.64	5
65	0.194±0.027		0.260: 0.296: 0.464	Present
	0.195		0.260: 0.276: 0.464	25
		0.19 ±0.02	0.00 : 0.36 : 0.64	6
		0.19	0.00 : 0.36 : 0.64	23
		0.195±0.014	0.00 : 0.36 : 0.64	24
		0.184±0.016	0.00 : 0.36 : 0.64	25

N_2: N_3 is not great enough to explain the discrepancies between the findings of Lay[3] at Z = 56, 57, and 59 using fluorescent x-ray excitation and the present work using radioactive sources. In experiments involving fluorescent excitation, the difficulties in accounting for scattered x rays and self-absorption of L x rays in the targets limit the accuracy. Moreover, with modern semiconductor x-ray detectors, much greater accuracy in relative x-ray intensity measurements is obtained than was available with the photographic plate method as used by Lay in 1934.

2) The measured values of $\bar{\omega}_L$ at Z = 57 by Hohmuth, Muller and Schintlmeister[4] and of ω_{KL} at Z = 59 by Hohmuth and Winter[5] based on measurements with gas proportional counters and NaI(Tl) scintillation spectrometers, are found to be lower than the present results. These discrepancies could be due to errors in the L x-ray efficiency in their work. It is not clear from their publications how the efficiency of the L x-ray detector was determined.

3) The values of ω_{KL} of Jopson, Mark, Swift and Williams[6] are larger than the present results for $\bar{\omega}_L$. It is possible that the corrections for the loss of L x rays in their foils is overestimated. The results of Jopson, Mark, Swift and Williams[6] were uncorrected for multiple vacancies. Lower values for ω_{KL} result from such a correction[7].

4) For Z = 55 there are no prior measurements.

5) All other work[6,22,25] seems to agree quite well with the present results*.

It is impossible to obtain an exact dependence of $\bar{\omega}_L$ on atomic number (Z) since $\bar{\omega}_L$ is a linear combination of six quantities which have a complex dependence upon Z (see eq. 2 p. 6).

3.4 Evaluation of I_{L_α}/I_{L_ℓ}

The ratio $(I_{L_\alpha}/I_{L_\ell})$ of the relative intensity of the $L_3 - M_{4,5}$ x-ray transition (I_{L_α}) to that of the $L_3 - M_1$ x-ray transition (I_{L_ℓ}) was determined with a high resolution Si(Li) detector from singles spectra for nuclides whose decay gives rise to x-ray transitions in nuclides of Z = 55, 57, 60, 65, 73, 82, 92, and 94.

The ratio of the counting rates of L_α and L_ℓ x-rays $(C_{L_\alpha}/C_{L_\ell})$ was determined by graphical integration for

---

*In the case of Z = 65 complete subshell information is available[25], so $\bar{\omega}_L$ can be calculated from this work using the equation:

$$\bar{\omega}_L = N_1\nu_1 + N_2\nu_2 + N_3\nu_3$$

where ν_1, ν_2, and ν_3 are the fraction of all L x rays observed per vacancy in the L_1 -, L_2 -, and L_3-subshells respectively. The value of $\bar{\omega}_L$ so calculated is 0.19, which compares with the present experimental value of 0.194 ± 0.027.

nuclides below Z = 65 and by numerical peak integration following subtraction of the continuum under the peaks above Z = 63, (see Fig. 4). The method of performing graphical integration consisted of subtracting continuous background under the L_α and L_ℓ full-energy-peaks from the L_α and the L_ℓ full-energy-peaks.

The intensity ratio I_{L_α}/I_{K_ℓ} was then calculated from the equation:

$$I_{L_\alpha}/I_{L_\ell} = (C_{L_\alpha}/C_{L_\ell})(\varepsilon_{L_\ell}/\varepsilon_{L_\alpha}) \qquad (13)$$

Experimental values of the ratio I_{L_α}/I_{L_ℓ} computed in this work are given in Table 5, where the error limits are twice the standard deviation (95 per cent confidence).

3.5 Discussion of the X-Ray Intensity Ratio I_{L_α}/I_{L_ℓ}

Table 6 lists values for the ratio I_{L_α}/I_{L_ℓ} from experiment and theory. Fig. 5 is a plot of the intensity ratio I_{L_α}/I_{L_ℓ} against Z for those values measured in the present work and those calculated by Scofield[26]. From this plot, it can be seen that the theoretical ratio I_{L_α}/I_{L_ℓ} of Scofield is consistently smaller (e.g. of the order of 15 per cent for $Z < 65$) than the present experimental results in the region of $55 \leq Z \leq 80$. The 15 per cent disagreement

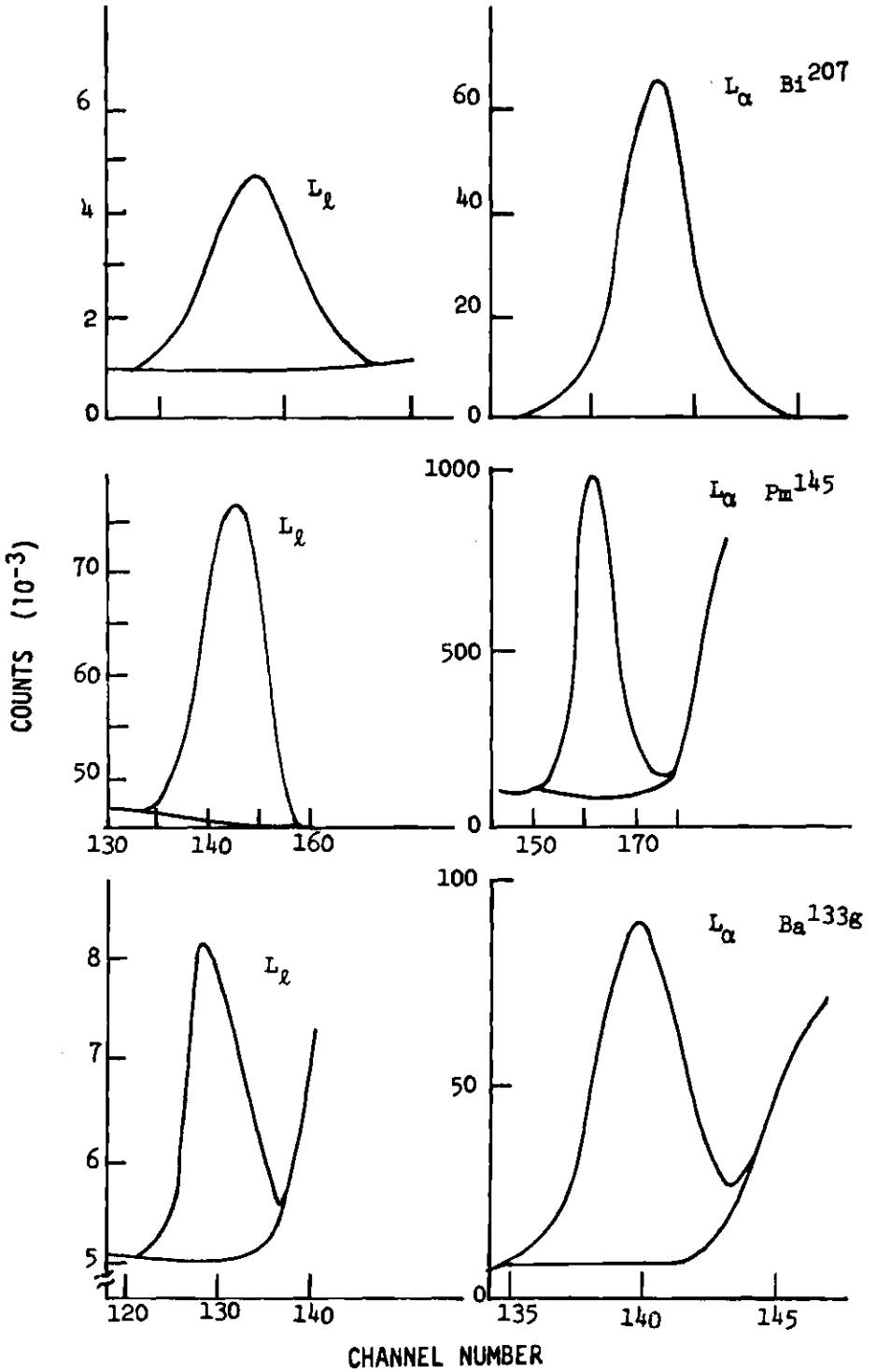

Fig. 4. Spectra Showing L_α and L_ℓ of Ba^{133g}, Pm^{145}, and Bi^{207}. (The estimated continuum is also shown.)

Table 5. The ratio (I_{L_α}/I_{L_ℓ}) of the Intensities of L_α-to-L_ℓ X Rays Originating from the Filling of L_3-Subshell vacancies as Measured in the Present Work.

Z	I_{L_α}/I_{L_ℓ}	Z	I_{L_α}/I_{L_ℓ}
55	31.5±2.0	73	23.7±1.0
57	31.1±2.0	82	20.1±1.0
60	28.8±1.8	92	15.0±1.0
65	26.1±1.5	94	15.6±1.0

Table 6. Ratio (I_{L_α}/I_{L_ℓ}) of the Intensities of L_α-to-L_ℓ X Rays Originating from the Filling of L_3-Subshell Vacancies.

Z	Experiment	Theory	Reference
51		26.4	26
55	31.5±2.0		Present
56		25.9	26
57	31.1±2.0		Present
60	28.8±1.8		Present
		25.1	26
63		24.4	26
65	26.1±1.5		Present
	26.2±1.8		28
		23.9	26
70	23.3±1.5		28
		22.7	26
		22.5	27
73	23.7±1.0		Present
	22.7±1.0		28
		21.8	26
74		21.3	26
77	23.8±2.0		28
78	20.8±1.0		28
		20.2	26
79		19.9	26
80		19.6	26
		19.5	27

(Continued)

Table 6. Ratio (I_{L_α}/I_{L_ℓ}) of the Intensities of L_α-to-L_ℓ X Rays Originating from the Filling of L_3-Subshell Vacancies (Continued)

Z	Experiment	Theory	Reference
81		19.2	26
82	20.1±1.0		Present
	20.5±0.5		28
		18.8	26
83	20.0±0.5		28
90		16.6	26
92	15.9±1.0		Present
	16.3±0.5		28
		16.1	26
93	16.4±0.5		28
		16.0	27
94	15.6±1.0		Present
	16.3±0.5		28

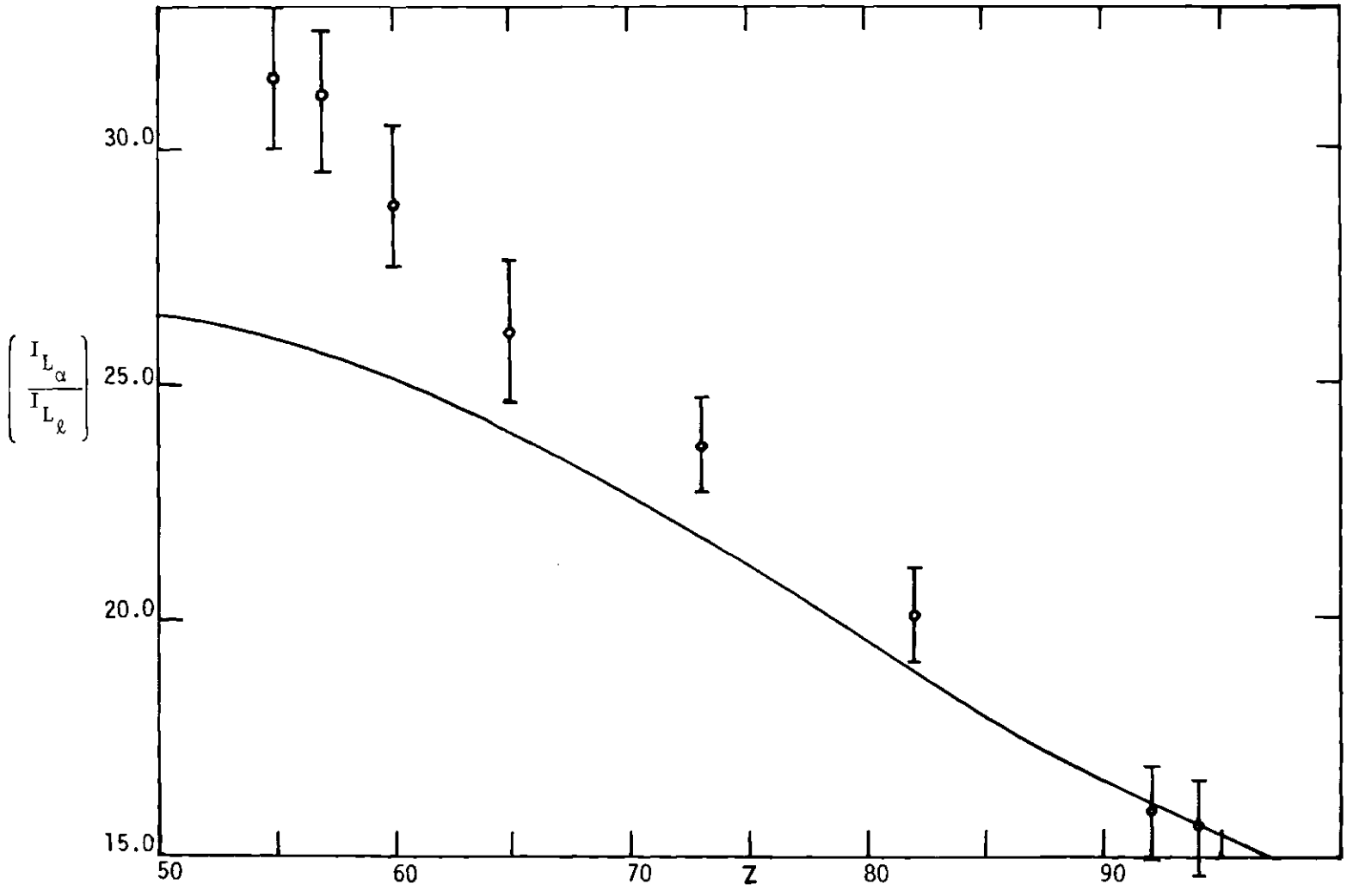

Fig. 5. Plot of the Ratio L_α/L_ℓ as a Function of Z. The solid curve is the theoretical one from Ref. 26.

is due to an overestimation of I_{L_ℓ} and/or an underestimation of I_{L_α} in Scofield's theory.

Since the ratio I_{L_α}/I_{L_ℓ} can be experimentally determined quite accurately, even a small error in the theoretical calculation of the L_ℓ or L_α x-ray intensity can be determined sensitively (e.g. to the order of 5 per cent).

The present results for I_{L_α}/I_{L_ℓ} agree with prior experimental results. Some of the results are measured in the present work for the first time (see Table 6). Discrepancies between experiment and theory such as those observed in the region of $50 \leq Z \leq 80$ are not evident at higher Z.

CHAPTER IV

CONCLUSIONS AND SUGGESTIONS

4.1 Conclusions

1) The measurements of $\bar{\omega}_L$ at Z = 56, 57, and 59 by Lay[3] are high compared to the present work (Sect. 3.3 and Table 4).

2) Values of $\bar{\omega}_L$ at Z = 57 by Hohmuth, Muller, and Schintlmeister[4] and of ω_{KL} at Z = 59 by Hohmuth and Winter are found to be lower than present results (Sect. 3.3 and Table 4).

3) Measurements of ω_{KL} uncorrected for multiple vacancies by Jopson, Mark, Swift, and Williams[6] are high compared to the present results for $\bar{\omega}_L$ (Sect. 3.3 and Table 4). After correction[7], these ω_{KL} values are in rough agreement with the present results for $\bar{\omega}_L$.

4) All results at Z = 65 agree very well (Sect. 3.3 and Table 4).

5) Disagreement between present experimental results and theory calculated by Scofield[26] is due to a possible underestimation of L_α and/or overestimation of L_ℓ (Sect. 3.5) in the theoretical calculations.

4.2 Suggestions For Further Work

Several additional experimental studies would enlarge our knowledge of L-shell fluorescence yields.

1) More accurate x-ray efficiency determinations should be made below 20 keV. Such determinations entail the development of ultra-thin low-energy radioactive x-ray standard sources, preferably prepared by electromagnetic isotope separation.

2) The quantity $\bar{\omega}_L$ should be determined accurately with mass-separated sources for nuclides of $Z < 55$, in order to eliminate uncertainties in source self-absorption.

3) The L-subshell fluorescence yields and Coster-Kronig transition probabilities should be studied by observing L x rays in coincidence with K_{α_1} x rays, K_{α_2} x rays, and L-conversion electrons for nuclides of $Z < 65$ and to atomic numbers as low as the improving detector resolution will permit in the future.

APPENDIX A

SAMPLE CALCULATION OF $\bar{\omega}_L$

The calculation of $\bar{\omega}_L$ for Ce^{139g} offers a good demonstration of the application of equations given in Sect. 1.4.

The decay scheme of Ce^{139g} is rather simple[14]. The nuclide Ce^{139g} decays by electron capture to the 166 keV excited state of La^{139} followed by a γ transition to the ground state.

The summations enclosed in brackets in eqs. 3 and 4 (see p. 7), namely $[\sum_n N_{K(n)} + \sum_{i,j} N_{K(i,j)}]$ and $[\sum_n N_{L(n)} + \sum_{i,j} N_{L(i,j)}]$, each contain a single term, since the decay scheme of Ce^{139g} contains one electron capture branch and one γ transition. The indices $\underline{n}$ and $\underline{i}$ are 166 while $\underline{j}$ is zero since Ce^{139g} electron captures to the 166 keV level of the daughter La^{139} which then γ decays to the ground state ($\underline{j}$) of La^{139}. Thus eqs. 3 and 4 assume the following form for Ce^{139g},

$$I_K = N_o \omega_K [N_{K(166)} + N_{K(166,0)}] \tag{14}$$

$$I_L = N_o \bar{\omega}_L [N_{L(166)} + N_{L(166,0)}] \tag{15}$$

where

$$N_{K(166)} = f_{(166)} P_{K(166)} \tag{16}$$

$$N_{K(166,0)} = b_{(166,0)} [\alpha_K/(1+\alpha_T)]_{(166,0)} \tag{17}$$

$$N_{L(166)} = f_{(166)} P_{L(166)} + n_{KL} N_{K(166)} \tag{18}$$

and

$$N_{L(166,0)} = b_{(166,0)} [\alpha_L/(1+\alpha_T)]_{(166,0)} + n_{KL} N_{K(166,0)} \tag{19}$$

It is possible to evaluate $N_{K(166)}$, $N_{L(166)}$, $N_{K(166,0)}$, and $N_{L(166,0)}$ from the following quantities calculated from previous work:

$P_{K(166)} = 0.730 \pm 0.011$ (using $P_{L+M}/P_K = 0.37$)[29]

$P_{L(166)} = 0.220 \pm 0.022$ (using P_K and $P_M/P_L = 0.21$)[30]

$[\alpha_K/(1+\alpha_T)]_{(166,0)} = 0.175 \pm 0.008$ (using $\alpha_K = 0.22$ and $K/(L+M) = 5.7$)[14]

$[\alpha_L/(1+\alpha_T)]_{(166,0)} = 0.0238 \pm 0.0024$ (using $K/L = 7.4$)[31]

$n_{KL} = 0.880 \pm 0.0024$ (details of calculations given in App. B)

The ratio of eqs. 15 and 14 gives an equation that can be then solved for $\bar{\omega}_L$; e.g.

$$\bar{\omega}_L = \omega_K (I_L/I_K) \{ [N_{K(166)} + N_{K(166,0)}]/[N_{L(166)} + N_{L(166,0)}] \} \tag{20}$$

Substitution of the quantities $N_{L(166)}$, $N_{L(166)}$, $N_{K(166,0)}$, and $N_{L(166,0)}$, ω_K (0.906 ± 0.014)[7] into eq. 20, and using the present measured ratio of $I_L/I_K = 0.139\pm0.014$ gives a value for $\bar{\omega}_L$ of 0.110 ± 0.015 for the decay of Ce^{139g}.

APPENDIX B

CALCULATION OF THE QUANTITY n_{KL}

The number of L-shell vacancies produced in the filling of a K-shell vacancy, n_{KL}, was calculated using eq. 9 for nuclides of Z = 55, 56, 57, 59, and 65. The ratio of I_{K_α}/I_K, was calculated from a tabulation of K_β/K_α given by Nelson, Saunders, and Salem[32]; ω_K was taken from Bambynek *et al.*[7]; and $[2(K\text{-}LL) + (K\text{-}LX)]/\Sigma$ Augers was calculated from graphs of (K-LX)/(K-LL) vs atomic number (Z) and (K-XY)/(K-LL) vs Z given in Siegbahn[33]. Addition of more recent values of (K-LX)/(K-LL) and (K-XY)/(K-LL) not contained in the plots given in Siegbahn had negligible effect on the curves of (K-LX)/(K-LL) vs Z and (K-XY)/(K-LL) vs Z. Table 7 gives the results of these calculations.

Tabel 7. The Number of L-Shell Vacancies Produced in the Filling of a K-Shell Vacancy for Several Atomic Numbers (Z = 55, 56, 57, 59, and 65), Calculated in the Present Work.

Z	n_{KL}	Z	n_{KL}
55	0.892±0.021	59	0.870±0.021
56	0.886±0.021	65	0.846±0.021
57	0.880±0.021		

APPENDIX C

EVALUATION OF PRIMARY VACANCY DISTRIBUTIONS

Since $\bar{\omega}_L$ is expressed in terms of the primary vacancy distribution $N_1 : N_2 : N_3$, the computation of this distribution is essential to the comparison of $\bar{\omega}_L$, measured in various experiments with different modes of vacancy excitation.

The equations for calculating the ratio $N_1 : N_2 : N_3$ are:

$$N_1 = n_1/(n_1 + n_2 + n_3) \tag{21}$$

$$N_2 = n_2/(n_1 + n_2 + n_3) \tag{22}$$

and

$$N_3 = n_3/(n_1 + n_2 + n_3) \tag{23}$$

where

$$n_1 = \sum_n f_{(n)} P_{L_1(n)} + \sum_{i,j} b_{(i,j)} [\alpha_{L_1}/(1+\alpha_T)]_{i,j} + n_{KL_1} N_{K(T)} \tag{24}$$

$$n_2 = \sum_n f_{(n)} P_{L_2(n)} + \sum_{i,j} b_{(i,j)} [\alpha_{L_2}/(1+\alpha_T)]_{i,j} + n_{KL_2} N_{K(T)} \tag{25}$$

and

$$n_3 = \sum_{i,j} b_{(i,j)} [\alpha_{L_3}/(1+\alpha_T)]_{(i,j)} + n_{KL_3} N_{K(T)} \tag{26}$$

where N_1, N_2, and N_3 are the normalized ($N_1+N_2+N_3 = 1$) primary vacancy distribution for the L_1, L_2, and L_3 subshells, respectively, and n_1, n_2, and n_3 are the number of vacancies produced by internal conversion and/or electron capture in the L_1, L_2, and L_3 subshells, respectively.

In complex decay schemes one often can neglect certain terms in the above equations. Since the n_{KL} contribution (ie. the shift of a K-shell vacancy to the L-shell) to the L-subshell vacancies is large in most cases (greater than 75 per cent of the total L vacancies produced for all nuclides studied here), one can neglect the contribution of vacancies produced from gamma-ray conversion of a transition between nuclear levels $\underline{i}$ and $\underline{j}$, $b_{(i,j)}[\alpha_{LX}/(1+\alpha_T)]_{(i,j)}$ for several cases in which $N_{L(i,j)}$ is small compared to $N_{L(T)}$. From Table 3 it is evident that the calculation of the primary vacancy distribution can be greatly simplified. The terms $b_{(i,j)}[\alpha_{LX}/(1+\alpha_T)]_{(i,j)}$ in the decay of Ba^{133g} can be neglected for all transitions except for those between the 437 and 382 keV levels, between the 81 keV level and the ground-state.

Table 8 gives the results of evaluation of the $N_1 : N_2 : N_3$ ratio for the decays of Ba^{133g}, Cs^{137}, Ce^{139g}, Ce^{141}, and Dy^{159}.

Primary vacancy distributions for ω_{KL} experiments are given by the following equations[18]:

$$N_1 = 0.00$$

$$N_2 = I_{K_{\alpha_2}} / I_{K_\alpha}$$

$$N_3 = I_{K_{\alpha_1}} / I_{K_\alpha}$$

where $I_{K_{\alpha_1}}$, $I_{K_{\alpha_2}}$, and I_{K_α} are the intensities of the K_{α_1} transition ($K - L_3$), K_{α_2} transition ($K - L_2$), and the total K_α transition ($I_{K_{\alpha_1}} + I_{K_{\alpha_2}} = I_{K_\alpha}$), respectively.

Table 8. Vacancy Distributions for Several Nuclides

Nuclide	Daughter	N_1: N_2: N_3
$_{56}Ba^{133g}$	$_{55}Cs^{133}$	0.252: 0.269: 0.479[a]
$_{55}Cs^{137}$	$_{56}Ba^{137}$	0.239: 0.275: 0.486[b]
$_{58}Ce^{139g}$	$_{57}La^{139}$	0.259: 0.266: 0.475[c]
$_{58}Ce^{141}$	$_{59}Pr^{141}$	0.233: 0.284: 0.483[d]
$_{66}Dy^{159}$	$_{65}Tb^{159}$	0.260: 0.276: 0.464[e]

[a] Calculated from data given in Refs. 11, 12, 13, and 34.

[b] Calculated from data given in Refs. 7, 20, and 35.

[c] Calculated from data given in Refs. 11, 29, 30, and 31.

[d] Calculated from data given in Refs. 14, 21, and 34.

[e] Calculated from data given in Refs. 11, 12, and 14.

BIBLIOGRAPHY*

1. P. Auger, J. Phys. Radium 6, 205 (1925).

2. H. G. Mosley, Phil. Mag. 26 1024 (1913).

3. H. Lay, Z. Physik 91, 533 (1934).

4. K. Hohmuth, G. Muller, and J. Schintlmeister, Nucl. Phys. 48, 209 (1963).

5. K. Hohmuth and G. Winter, Phys. Letters 10, 58 (1964).

6. R. C. Jopson, H. Mark, C. D. Swift, and M. A. Williamson, Phys. Rev. 131, 1165 (1963); Bull. Am. Phys. Soc. 8, No. 1, 49 (1963) 7, 491 (1962).

7. W. Bambynek, B. Crasemann, R. W. Fink, H. U. Freund, Hans Mark, R. E. Price, P. V. Rao and C. D. Swift, (to be published in Rev. Mod. Phys.); reprint (1971).

8. H. U. Freund, J. S. Hansen, E. Karttunen and R. W. Fink, Proc. Int. Conf. on Radioactivity in Nuclear Spectroscopy, Nashville, Tennessee, 1972 (Gordon and Breach Publ., New York).

9. J. S. Hansen, Ph.D. Dissertation, Georgia Institute of Technology, Atlanta, Georgia (1971) (Unpublished).

10. J. S. Hansen, J. C. McGeorge, H. U. Freund, W. D. Schmidt-Ott, D. W. Nix, I. Q. Unus, and R. W. Fink (in progress).

11. M. J. Martin and P. H. Blichert-Taft, Nucl. Data A8, 157 (1970).

12. R. W. Hager and E. C. Seltzer, Internal Conversion Tables, Part I K, L, M-shell Conversion Coefficients, Nucl. Data A4, 1 (1968).

13. W. D. Schmidt-Ott and R. W. Fink, Z Physik (in press) (1972).

*Abbreviations used herein follow the form employed by the American Institute of Physics Style Manual, published by the AIP Publication Board, 2nd edition, 1959.

BIBLIOGRAPHY (Continued)

14. C. M. Lederer, J. M. Hollander and I. Perlman, Table of Isotopes, 6th ed. (John Wiley and Sons, Inc., New York, 1967).

15. J. R. Rhodes, (ASTM Special Technical Publications Rept. No. STP 485) (1971), pp. 243 - 285.

16. D. W. Aitken, (Rept. No. AFOSR 69 - 1867 TR) (1969).

17. R. G. Jaeger, editor, Engineering Compendium on Radiation Shielding Volume I, (Springer - Verlag, New York, 1968) 184.

18. R. W. Fink, R. C. Jopson, Hans Mark and C. D. Swift, Rev. Mod. Phys. 38, 513 (1966).

19. E. I. Karttunen, Ph.D. Dissertation, Georgia Institute of Technology, Atlanta, Georgia (1971) and E. I. Karttunen, H. U. Freund, and R. W. Fink, Phys. Rev. A4, 1695 (1971).

20. H. H. Hansen, G. Lowenthal, A. Spernol, W. Van Der Eijk, and R. Vaninbroukx, Z. Physik 218, 25 (1969).

21. C. B. Zorzoli, Nuovo Cimento V, N. 1, 289 (1957).

22. H. W. Beste, Z. Physik 213, 333 (1968).

23. N. H. Lazar and W. S. Lyons, Bull. Am. Phys. Soc. 3, No. 1, 29 (1958).

24. A. A. Konstantinov and T. E. Sazanova, Proc. Symp. Standardization of Radionuclides, Oct. 1966, Vienna, (International Atomic Agency, Vienna, 1967) pp. 357ff.

25. J. C. McGeorge, H. U. Freund, and R. W. Fink, Nucl. Phys. A 154, 526 (1970).

26. J. H. Scofield, Phys. Rev. 179, 9 (1969).

27. H. R. Rosner and C. P. Bhalla, Z. Physik 231, 347 (1970); Supplementary Tables NAPS Document No. 00739 (National Auxiliary Publications Service, New York, 1969).

28. P. V. Rao, J. M. Palms, and R. E. Wood Phys. Rev. A3, 1568 (1971).

BIBLIOGRAPHY (Continued)

29. B. H. Ketelle, H. Thomas, and A. R. Brosi, Phys. Rev. 103, 190 (1956).

30. J. P. Renier, H. Genz, K.W.D. Ledingham, and R. W. Fink, Phys, Rev. 166, 935 (1968).

31. J. S. Geiger, R. L. Graham, and I. Bergström, Nucl, Phys. 68, 352 (1965).

32. G. C. Nelson, B. G. Saunders, and S. I. Salem, Atomic Data 1, 377 (1970).

33. K. Siegbahn, editor, Alpha, Beta and Gamma Spectroscopy, (North Holland Publ. Co., Amsterdam, 1964).

34. P. V. Rao, M. H. Chen, and B. Crasemann, Atomic Vacancy Distributions Produced by Inner-Shell Ionization, (submitted to Physical Review A, 1971).

35. L. J. Velinsky, Ph.D. Dissertation, Michigan State University, East Lansing, Michigan (1965) (unpublished); Nucl. Sci. Abstr. 20, 11143 (1966).